Comprehensive Approach to Improve Backflashover Rate in Overhead Transmission Lines Using Top and Multiple Underbuilt Wires

J. E. Guevara Asorza, J. S. Leon Colqui, J. Pissolato Filho

***Abstract*—This paper presents a technical evaluation of using top wires (TW) and multiple underbuilt wires (UW) to improving the backflashover rate of a typical 220 kV transmission line installed over high-resistivity soil (5000 Ω.m). The study first assesses the impact of installing UWs across several spans, which proved to be ineffective in significantly reducing overvoltages on the insulator string. To address this inefficiency, two alternative solutions were considered: install multiple UWs, as a bundle, and another, proposed in this work, that combines TWs and UWs. Both strategies reduced the impact area and the number of affected towers, with the combined approach demonstrating superior performance. Additionally, increasing the UW cross-section had a negligible effect on overvoltage reduction while introducing unnecessary structural stress and in contrast, increasing the TW cross-section significantly improved performance in mitigating overvoltages. These findings highlight the effectiveness of combining TWs and UWs as a more robust solution for enhancing the lightning performance of transmission lines, particularly in high-resistivity soil conditions.**

***Keywords*—Backflashover rate, lightning performance, transmission line, top wire, underbuilt wire.**

I. Introduction

THE performance and reliability of overhead transmission lines (OHTLs) are fundamental to the efficient operation of power systems. As the demand for electrical energy continues to rise, ensuring the resilience of these lines becomes increasingly critical. Lightning strikes are a significant source of disruptions in OHTLs, often causing backflashovers (BFs) and power outages with severe economic and social impacts [1]. Therefore, implementing effective protective measures minimizes these effects and ensures system stability [2].

In order to mitigate the impact of lightning on OHTLs, various techniques are employed [2]–[5], including installing surge arresters, additional shield wires, enhancements to grounding systems, and adding underbuilt wires (UWs) beneath the phases of OHTLs. In the past decade, the use of UWs has gained considerable attention due to their effectiveness in reducing BFs.

This paper was supported by the São Paulo Research Foundation (FAPESP) grants: 2021/11258-5, 2021/06157-5, 2023/05066-1 and 2024/14472-6. J. E. G. Asorza is with the School of Electrical and Computer Engineering, University of Campinas - UNICAMP, Campinas, Brazil, (e-mail of corresponding author: j272296@dac.unicamp.br). J. S. León the School of Electrical and Computer Engineering, University of Campinas - UNICAMP, Campinas, Brazil (e-mail: jaimis@unicamp.br). J. P. Filho is with the School of Electrical and Computer Engineering, University of Campinas - UNICAMP, Campinas, Brazil, (e-mail: pisso@unicamp.br).

Paper submitted to the International Conference on Power Systems Transients (IPST2025) in Guadalajara, Mexico, June 8-12, 2025.

However, there are still gaps in the literature regarding various aspects of UW usage, such as the number of spans in transmission towers where they can be applied, their relationship with the amplitude of the lightning discharge current, and the current wave reflections. Additionally, when it is economically unfeasible to further reduce tower footing resistance or limit voltage across insulator strings through surge arresters due to the cost of arresters, installation and maintenance complications, and space constraints in compact line designs, there is a strong justification for seeking alternative solutions.

Enhancing the electromagnetic coupling with the phase conductors is one promising method of lowering overvoltages on insulator strings. Positioning a top wire (TW) near the shield wires, above the phase conductors, can be accomplished. TWs enhance coupling and lower the equivalent surge impedance at the top of the tower, giving lightning current another low-impedance path.

In this context, this work contributes to this topic through a technical analysis of TWs and UWs for improving lightning performance in transmission lines, especially the backflashover rate (BFR). It details the role and effectiveness of each technique under varying conditions, including lightning amplitude, number of spans, multiple conductors, and cross-sectional dimensions of TWs and UWs.

II. Modeling the Power System Elements

A. Computing electrical parameters for an OHTL

Two full-wave formulations exist in the literature [6]–[8], developed using the electric scalar potential and the magnetic vector potential for computing earth-return impedance and admittance. These formulations are commonly referred to as the potential and voltage formulations, where the last is the most rigorous and physical formulation. The first establishes a remote ground for potential reference, while the latter calculates the voltage between the overhead conductor and the surface of the soil. The difference in results between these formulations in lightning studies is evident [9]. In this work, the voltage formulation was employed. The calculation of the parameters for this approach is described as follows:

$$Z = Z_{int} + \frac{j\omega\mu_0}{2\pi}\left(P + S_1 - (S_2 + S_3)\right) \tag{1}$$

$$Y = j\omega\varepsilon_0 2\pi \left(P - S_3\right)^{-1} \tag{2}$$

where P, S_1, S_2, and S_3 are functions defined by infinite integrals, as detailed in [6]–[8]. Additionally, μ_0 represents the permeability of free space, ε_0 denotes the permittivity of free space, and ω represents the angular frequency in rad/s.

B. Frequency-dependent soil model

Soil is composed of organic matter, minerals, water, and gases. From an electrical perspective, soil can be characterized by its conductivity (σ_g), dielectric permittivity (ε_r), and magnetic permeability (μ), with the latter assumed to be equal to μ_0. According to [10], both σ_g and ε_r are highly influenced by frequency within the range of lightning phenomena and should therefore be considered in studies of overvoltages caused by lightning strikes. This study examines the frequency-dependent behavior of soil's electrical parameters using a causal physical model proposed by Alipio-Visacro [11]. These parameters are given by:

$$\sigma_g(f) = \sigma_0 \left\{1 + 4.7 \cdot 10^{-6} \cdot \sigma_0^{-0.73} \cdot f^{0.54}\right\} \tag{3}$$

$$\varepsilon_r(f) = 12\,\varepsilon_0 \cdot 10^{-4} \cdot \sigma_0^{0.27} \cdot f^{-0.46} \tag{4}$$

where σ_0 is the low-frequency soil conductivity (measured at low frequencies), and f is the cyclic frequency.

C. Tower model

The revised Jordan's formula was used to calculate the tower surge impedance. This formula approximates the apparent propagation speed along the tower as about 80% of the speed of light, as detailed in [12], taking into account the tower sections and cross arms. According to [13], this model aligns well with the Hybrid Electromagnetic Model (HEM). In this work, we determined the equivalent impedance values, Zeq_i, using the following expressions:

$$Z_{i,i} = Z_{ii} = 60\,ln\left(\frac{4h}{r}\right) - 60 \tag{5}$$

$$Z_{i,j} = 60\,ln\left(\frac{2h + \sqrt{4h^2 + d_{ij}^2}}{d_{ij}^2}\right) + 30\frac{d}{h} - 60\sqrt{1 + \frac{d_{ij}^2}{4h^2}} \tag{6}$$

$$Zeq_i = \frac{Z_{i1} + Z_{i2} + Z_{i3} + ... + Z_{in}}{n} \tag{7}$$

where h represents the height in meters, d_{ij} denotes the distance in meters between conductors i and j (main chords), r stands for the radius of the main chord, and n indicates the number of main chords. The calculated values are Zeq_4 = 217.69 Ω, Zeq_3 = 215.38 Ω, Zeq_2 = 210.28 Ω and Zeq_1 = 131.7 Ω. This last one was divided in two parts: the first one is 34.78 Ω that represents the part of the tower measured from the last cross arm to the location of the UW and 96.9 Ω represents the rest of the structure. Furthermore, the impedance values for the cross arms, including those supporting the shield wires, are 173.03 Ω. The representation of each mentioned part of the tower and its respective equivalent impedance values will be presented along with the silhouette in Section III.

D. Grounding system for the tower

The grounding system plays a crucial role in lightning studies. To determine the harmonic impedance $Z(\omega)$ of the grounding system, we used the Hybrid Electromagnetic Model (HEM) [14], which is considered an accurate approach in the frequency domain. The impedance $Z(\omega)$ of the tower-footing grounding is determined over a frequency range from DC to several MHz, and it taking into account the frequency-dependent electrical characteristics of the soil [11].

E. Insulator string model

In this study, the voltage-time (V-T) model was utilized for the insulator string, focusing solely on the length of the insulator string to assess its voltage withstand capability (V_{FO}), as described in [15] and [16]. If a lightning overvoltage exceeds the V-T curve, a BF is likely to occur. The formula for determining V_{FO} is provided in equation (8).

$$V_{FO} = \left(400 + \frac{710}{t_c^{0.75}}\right)\ell \tag{8}$$

where t_c represents the flashover time, and ℓ denotes the length of the insulator string from the energized point to the ground.

It is important to note that the V–T model is a simplified approach, primarily valid for standard impulse waveforms, and less accurate than leader progression models. However, as this study focuses on evaluating the BFR in configurations with UW and TW, rather than on modeling accuracy, the simplified approach was deemed appropriate.

F. Lightning current model

The lightning current waveform impacting the OHTL was modeled as a combination of seven Heidler functions [17], based on data from the Morro do Cachimbo Stations [18]. The lightning waveform is expressed as follows:

$$i(t) = \sum_{k=1}^{N} \frac{I_{0k}}{\eta_k} \frac{(t/\tau_{1k})^{n_k}}{1 + (t/\tau_{1k})^{n_k}}\, e^{(-t/\tau_{2k})} \tag{9}$$

$$\eta_k = \exp\left[-\left(\frac{\tau_{1k}}{\tau_{2k}}\right)\left(n_k \frac{\tau_{2k}}{\tau_{1k}}\right)^{\frac{1}{n_k}}\right] \tag{10}$$

where I_{0k} regulates the amplitude, τ_{1k} represents the time constant related to the front time, τ_{2k} is the decay time constant, η_k is the amplitude correction factor, and n_k is the exponent that dictates the slope of each component k used to construct $i(t)$.

III. Results

This section presents the results of implementing TW and UW in a 220 kV OHTL subjected to lightning strikes, particularly impacting the tower. The study is structured into three subsections. The first subsection presents a comprehensive analysis of the overvoltages generated by five distinct lightning current waveforms, as listed in Table I, under scenarios involving the implementation of TW and UW. The second one offers a detailed comparative discussion on the performance and implications of employing TW and UW. Finally, the third subsection evaluates the resulting

improvements in the BFR associated with using TW and UW based on the scenarios examined in the first section. For all the cases, only one high electrical resistivity of the soil, 5000 Ω·m, is considered. Furthermore, the soil parameters, including electrical resistivity and permittivity, take into account their dependence on frequency.

The grounding system for the transmission towers is shown in Fig. 1, where all elements are copper-clad steel. The system's dimensions, detailed in Table II, were used to calculate the impedance magnitude and phase in the frequency-domain, as presented in Fig. 2. The 220 kV OHTL, as detailed in Fig. 3, consists of three AAAC conductors, two shield wires, an optical ground wire (OPGW), and extra high strength (EHS), with specifications outlined in Table III.

TABLE I: Lightning waveform (WF) used in the study

Multiplier/Parameter	WF 1	WF 2	WF 3	WF 4	WF 5
$Ip1$ (kA)	80.81	101.01	121.21	141.41	161.61
$Ip2$ (kA)	91.35	114.19	137.03	159.87	182.71
$T30$ (μs)	3.00	3.00	3.00	3.00	3.00
$T10$ (μs)	5.22	5.22	5.22	5.22	5.22
$T50$ (μs)	53.8	53.8	53.8	53.8	53.8

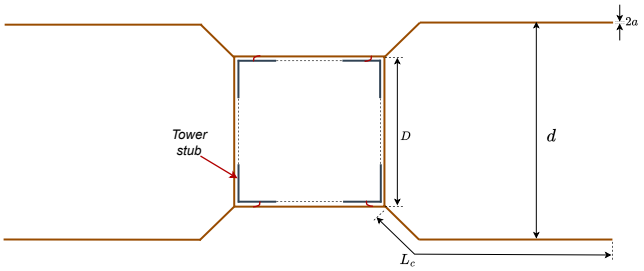

Fig. 1: Grounding system utilized.

TABLE II: Data of the grounding system

Description	Unit	Value
L_c	m	15
a	mm	5.5
d	m	30
D	m	11

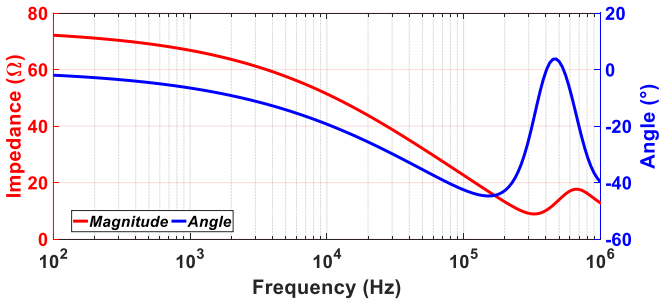

Fig. 2: Magnitude and phase impedance of the grounding system

For all transient response simulations, the PSCAD/EMTDC® software [19] was used . In this software, all power system components were represented using the models indicated in Section II. Below, some details of these models are provided.

To compute the electrical parameters of the OHTL, this paper uses the voltage formulation presented in Section II-A

TABLE III: Data for the OHTL at 220 kV

Description	Unit	Value
Type of conductor	-	AAAC 1000 kcmil
Conductor external diameter	mm	29.27
Conductor internal diameter	mm	0.0
Conductor resistance in DC - 20°C	Ω/km	0.06627
Conductor weight	kg/km	1390.0
Conductor sag	m	14.33
Conductor rated strength	kg	14905
Type of EHS	-	EHS 7/16"
EHS external diameter	mm	11.11
EHS Resistence in DC - 20°C	Ω/km	2.815
EHS weight	kg/km	593.6
EHS rated strength	kg	9431.5
Type of OPGW	-	AlumaCore - AFL
OPGW external diameter	mm	14.5
OPGW internal diameter	mm	9
OPGW Resistence in DC - 20°C	Ω/km	0.441
OPGW weight	kg/km	611.4
Average span	m	430

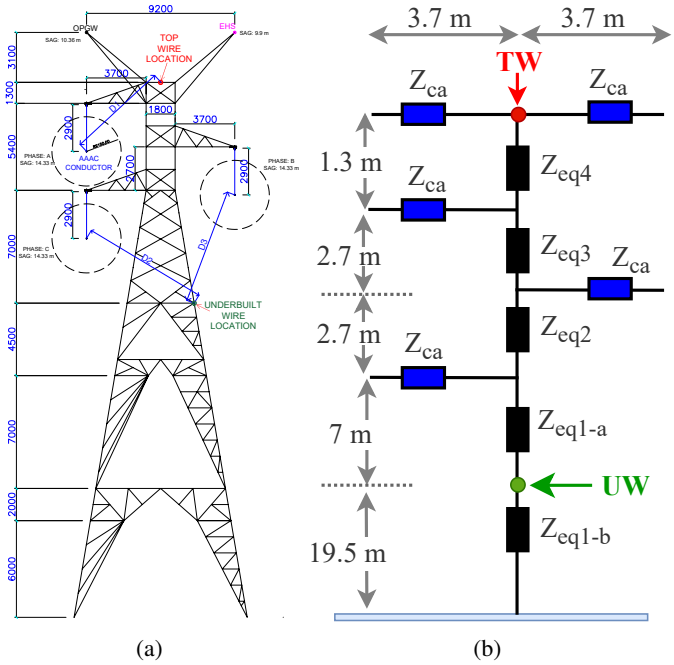

(a) (b)

Fig. 3: (a) Silhouette of a 220 kV tower and (b) its corresponding PSCAD model.

and considers the soil parameters as frequency-dependent, based on the experimental formulation developed by Alipio-Visacro [11]. Using this approach, we calculated the series impedance and shunt admittance matrix of the OHTL in the frequency domain, from 0.01 Hz to 1 MHz. These calculations were performed using MATLAB, and the resulting parameters—series impedance and shunt admittance in the frequency domain—were then imported to PSCAD/EMTDC using the Manual Data Entry component. Additionally, this software uses the Universal Line Model [20] to model the OHTL, providing a comprehensive and accurate frequency-dependent model by fitting the propagation matrices H and the characteristic admittance Yc in the phase domain.

For tower modeling, each element was modeled using the Bergeron line model [5], with the input data including surge impedance, length, and propagation speed [21]. The surge

impedance and length were determined in Section II-C, and the tower representation with these data is shown in Fig. 3b. The propagation speed is assumed to be 80% of the speed of light in a vacuum [12]. For the harmonic impedance $Z(\omega)$ of the grounding system, calculated as indicated in Section II-D, we represented it using the FDNE block in PSCAD to simulate the dynamic behavior of the grounding system. For the insulator string, the V-T curve is implemented using basic control blocks in PSCAD, forming a logical diagram, as referenced in [22].

Additionally, it is considered the aspects discussed in CIGRE 839 [1] to conduct the lightning study, including the tower surge impedance, representation of the lightning stroke, the number of towers involved, the insulator string model with a length of 2.4 meters, and the inclusion of the power frequency source at different angles. For the overvoltage simulations, an angle of 60° was adopted. In contrast, calculating the critical current required for the BFR considered twelve different angles, with a step of 30° [23].

Fig. 4 presents the system implemented in PSCAD/EMTDC, considering two spans forward and back with UW. For this study, we considered the UW that produces the lowest mechanical load to the tower; in that sense, we selected the EHS 3/8" wire, according to the Table IV, adapted from [24].

TABLE IV: Technical details of the extra high strength wires

Description	Unit	UW1	UW2	UW3	UW4
Type of EHS	-	3/8"	7/16"	1/2"	5/8"
Section	mm^2	51.10	75.6	96.58	152.00
External diameter	mm	9.14	11.11	12.57	15.77
Resistance in DC - 20°C	Ω/km	4.12	2.82	2.23	1.38
Weight	kg/km	406.1	593.6	769.1	1209.5

A. Overvoltages results

In the following simulations, we presented the overvoltages measured in the insulator strings when an atmospheric discharge strikes the tower through the OPGW, using the current waveforms indicated in Table I. The objective of each simulation is to prevent BF event, for the specific WF, by employing both TW and UW.

When the first current waveform strikes the OHTL, a BF occurs in phase B due to the second peak of the overvoltage wave when the UW is not installed. To prevent this BF, the installation of a UW is necessary. The UW reduces the first peak of the overvoltage wave in all three phases by approximately 0.25 MV. As the first peak decreases, the next peaks also decrease and do not produce BF, as shown in Fig. 5.

On the other hand, Fig. 6 presents the overvoltage waveform in the insulator string when the WF2 strikes into the OHTL. Three cases are analyzed in this figure, which is when the OHTL does not have UW, when it has UW installed in one span forward and back (two in total, 2S), and last when the UW is installed in two spans forward and back (four in total, 4S). In this last scenario, the BF event for this specific WF is eliminated. Without UW, BF happens in phases B and C. In the scenario where the UW is installed in one span forward and back, the first peak of the overvoltage in the phases decreases by approximately 180 kV. However, at the third peak of the wave, the reflected wave—originating from the wave traveling in the UW—exceeds the voltage-time characteristic curve of the insulator string, leading to a BF in phase B, for this specific WF. At this moment, the overvoltage in the other phases decreases and will not produce more BF. In other words, in this scenario, the problem is the reflection of the wave that travels in one span, so when the number of spans increases, it must be better. Therefore, in the third case, the overvoltage is analyzed when the UW is installed two spans forward and two spans back 4S. As expected, increasing the number of spans helps reduce overvoltages, especially when compared to the second scenario. This effect becomes more noticeable in the later voltage peaks—for example, in phase B, the first peak drops by 19 kV, while the second sees a larger drop of 41 kV. Thanks to this reduction, the overvoltage in phase B stays below the V-T curve, effectively preventing a BF event.

As the lightning amplitude increases, more spans are needed to prevent BF. However, the UW reaches a saturation limit beyond a certain point and can no longer effectively mitigate BFs—even with multiple installations along the OHTL. For example, Fig. 7 presents the overvoltage in the insulator string in three scenarios when WF3 strikes into the OHTL. The first one is the line without UW, where, for this WF, BF occurs in two phases. The second scenario, where the UW is installed in two spans (one forward and the other one in the back, 2S), occurs BF in one phase. The last case consists of installing UWs in 16 spans (16S); however, the BF in phase B still occurs.

The BF problem in this simulation differs from previous cases, where it was caused by the second or third peak of the overvoltage wave. In this case, the critical issue lies in the first peak. Although the UW helps reduce this peak, the mitigation is insufficient, and BF still occurs for this WF.

When installing UWs along the line becomes ineffective and logistically challenging—requiring civil and structural validation for different towers—an alternative is to increase the UW cross-section. However, as shown in Fig. 8, BFs may still occur if the first peak amplitude is too high, even with a larger cross-section. Therefore, the UW cross-section, increased as shown in Table IV, had minimal impact on overvoltage reduction.

Another alternative solution is to introduce the use of a TW. In this case, we located this wire between the shield wires in the middle of the tower, as we can see in Fig. 3. When the TW is considered, and one UW is installed in two spans forward and back (4S), it is possible to reduce the first peak of the overvoltage, as Fig. 9 shows. Nevertheless, the BF, for this WF, still occurs in phase B in the third peak of the overvoltage. To reduce this peak, as we demonstrated in previous simulations, it is necessary to install a UW; however, one is already in the tower. Therefore, an additional UW should be installed adjacent to the existing one, spaced approximately 50 to 60 centimeters apart. Both UWs should be connected to the tower at the same point using triangular yokes; meanwhile, spacer yokes must be used to guarantee this separation along the spans.

Considering two UWs and one TW installed in four spans in total (2 forward and 2 back, 4S), the overvoltage in all the phases decreases, as we appreciated in Fig. 10. It is important

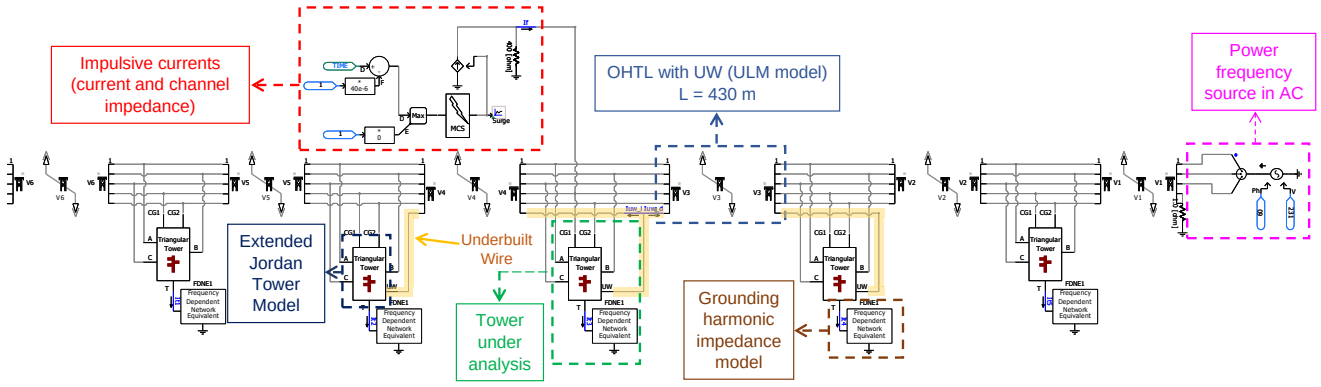

Fig. 4: System analyzed in PSCAD with one UW in two spans

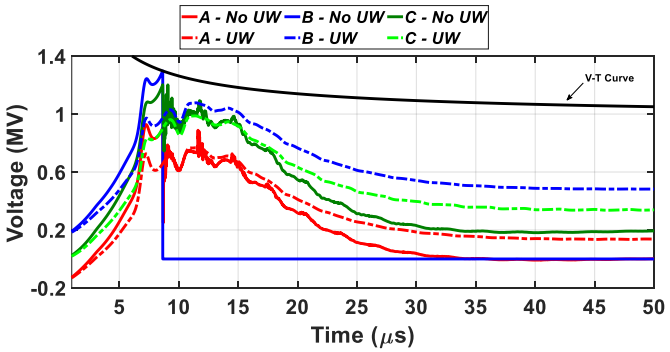

Fig. 5: Overvoltage in the insulator string with and without UW for WF1

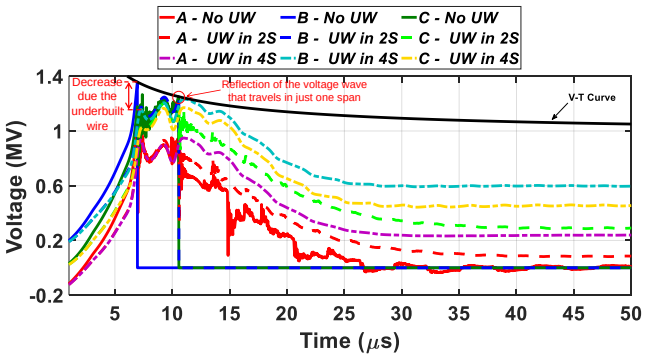

Fig. 6: Overvoltage in the insulator string with and without UW for WF2

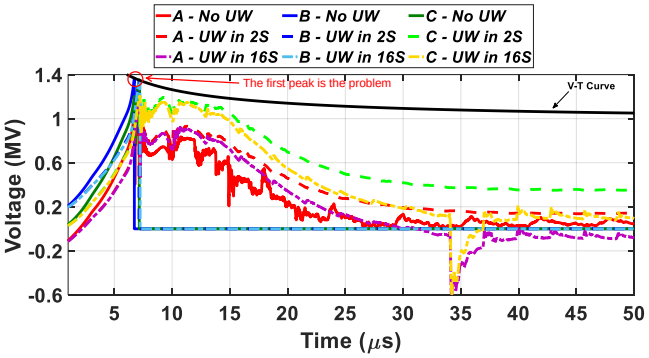

Fig. 7: Overvoltage in the insulator string with and without UW for WF3

to highlight that the TW used in the simulations is the same EHS (7/16") installed on the OHTL as shield wire, because it

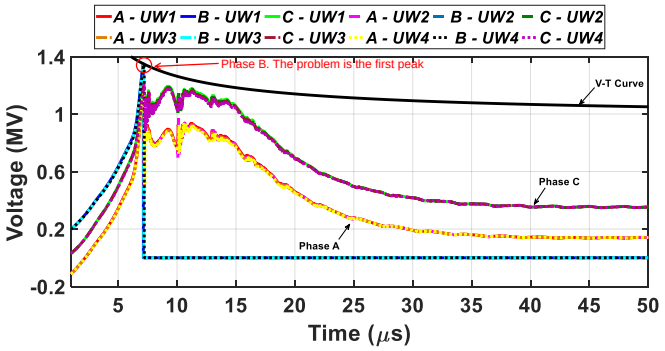

Fig. 8: Overvoltage in the insulator string with WF3 increasing UW section

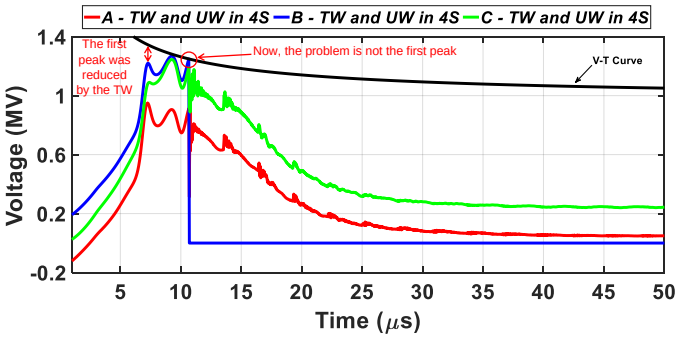

Fig. 9: Overvoltage in the insulator string with one TW and one UW for WF3

is susceptible to atmospheric discharges since it is positioned at the top of the OHTL. In order to maintain the reliability of the OHTL, this wire must be dimensioned at least to the same specifications as the other shield wire installed. With this alternative, we used twelve wires and successfully eliminated BF. In contrast, as shown in Fig. 7, installing sixteen UWs required more wires but still failed to resolve the BF issue.

In order to avoid event when the amplitude of lightning waveform strikes into the tower increase, two UWs with one TW is not enough. In this scenario, it is necessary to increase the number of UWs, getting finally four UWs in a quadrangular configuration with a separation of 50 - 60 cm. For example, in the simulation where the WF4 strikes into the tower, it is easy to note that when two UWs with one TW are installed, a BF occurs in phase C. Nevertheless, if we increase the number of sub-conductors of UW to four, we eliminate the

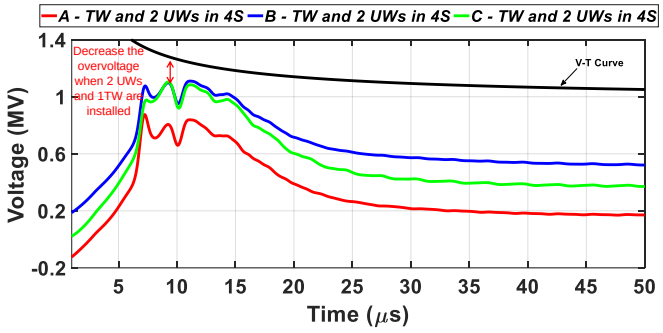

Fig. 10: Overvoltage in the insulator string with one TW and two UW for WF3

BF event for this WF, in this phase, as we show in Fig. 11.

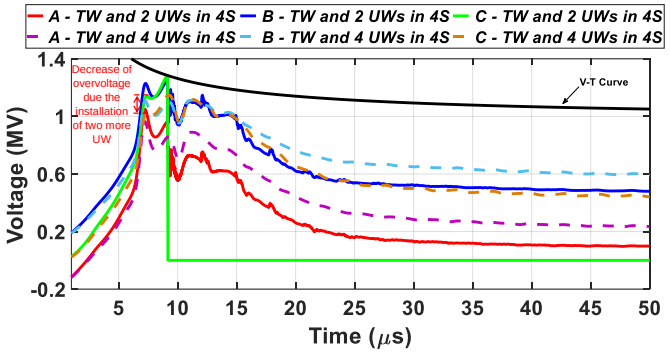

Fig. 11: Overvoltage in the insulator string using multiples UWs with TW

When WF5, the highest value of the amplitude of lightning waveform considered, occurs and strikes in the OHTL, the alternative of installing four UWs with one TW in four spans in total is not enough to eliminate the BF. In that sense, it is necessary to increase the cross-section of the TW from EHS 7/16" (TW1) to EHS 1/2" (TW2). Changing the cross-section of the TW decreases the first peak of overvoltage to approximately 58 kV, and as the first peak decreases, the second will also decrease and will not cross the V-T curve of the insulator string. This decrease is well explained in the Fig. 12. Increasing the number of UWs from four to five would add 174.6 kg of weight, while increasing only the cross-section of the TW adds just 75.5 kg. Therefore, the latter option was chosen as the preferred alternative.

Moreover, it is important to note that since the TW is closer to the lightning strike point, it experiences higher overvoltages and overcurrents. Increasing its cross-sectional area lowers its resistance, enabling more surge current to flow through it and more effectively mitigating the overvoltage reaching the insulator string. Although the UW serves a similar purpose, its position beneath the phase conductors results in lower surge current and voltage diversion. Thus, while increasing the UW's cross-section improves performance, the impact is less significant than the TW. Additionally, the TW is more effective in attenuating the first peak of the surge, whereas the UW mainly reduces the reflected wave from the grounding system. Both contribute to decreasing the overvoltage stress on the insulator string.

After five simulations with varying lightning amplitudes,

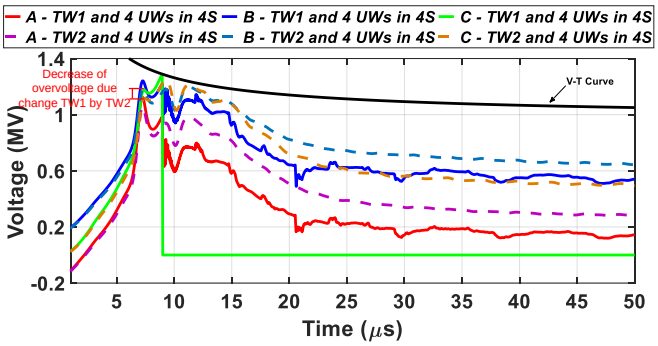

Fig. 12: Overvoltage in the insulator string using multiples UWs and different TW

BFs were successfully eliminated for these specific waveforms. This analysis is essential, especially when grounding improvements or surge arresters are not feasible. On the other hand, to better assess the actual lightning performance of the TW and UW configurations, a BFR calculation is necessary. This analysis is presented in Section III-C.

B. Difference between TW and UW

The first discussion topic is whether the TW is always necessary or whether it is better to install UW or TW. In order to address this question, it is necessary to try to solve the problem of eliminating the BF in the OHTL when the WF3 is analyzed. In this simulation, the option that successfully eliminates BF event is the installation of two UWs and one TW. However, we also considered the scenario of installing three UWs instead. The Fig. 13 presents this analysis, showing that both alternatives effectively prevent BF. However, when comparing overvoltages, we found that the TW + two UWs option results in lower overvoltages than the three UWs option. For instance, at the first peak, the difference is approximately 60 kV. This indicates that the TW + UWs configuration is more effective and attractive than using UWs alone.

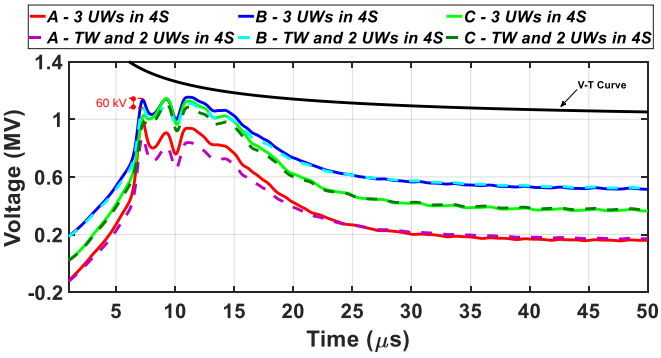

Fig. 13: Overvoltage in the insulator string using UWs vs TW with UWs

On the other hand, installation TW and UW must be analyzed from the following points of view: insulation coordination, mid-span clearance, civil, and structural. The first one, the insulation coordination, the distance D1, D2, and D3 showed in Fig. 3 have to satisfy the minimum distance calculated using the formulations indicated in the IEC 60071-1 [25] and IEC 60071-2 [26]. For this study, the minimum

distance is 2.15 m, which corresponds to the phase-to-ground clearance for fast-front overvoltage. Regarding mid-span clearance, it is essential to evaluate this distance using the empirical formulations suggested in [27], which consider the swing angle of the insulator string. For the UW, it is necessary to validate the safety distance of this wire to the ground. Finally, to ensure that all clearance distances meet the required standards, it is necessary to create a template for the towers involved in the study and validate these distances under various environmental and wind conditions. For this purpose, software such as PLS-CADD [28] can be utilized. Civil and structural considerations are critical for the installation of TW and UW [5]. All steel components must be thoroughly analyzed, as they are subject to pollution, oxidation, loosening of bolts, and other factors. Additionally, due to the increased mechanical loads, a review of the tower's foundations is also essential.

C. Backflashover analysis

Considering twelve different power frequency angles, the critical current, I_c, was calculated for the scenarios described in Section III-A. Fig. 14 illustrates the increase of the I_c when a UW is installed, compared to the reference case without a UW. As expected, the lowest I_c occurs in the phase closest to ground, phase C, and when its voltage reaches its steady-state peak, corresponding to a 150° angle. On the other hand, the higher value of I_c occurs in the phase A, which is the phase A located farther to the ground. Furthermore, on average, the presence of the UW results in a 35 % increase in the I_c.

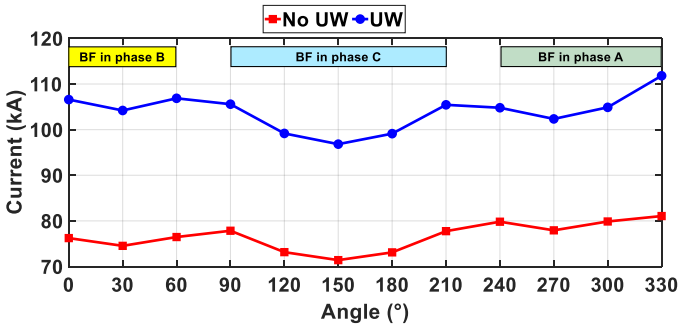

Fig. 14: I_c with and without UW

Fig. 15 shows the I_c for scenarios with UW installed over two and four spans. Increasing the number of spans to four results in an average increase of 6% in the I_c. Alternatively, installing TW and UW over just two spans—using the same number of wires from the case UW in 4S—yields an 11% increase compared to the UW in 2S. When both TW and UW are installed across four spans, the I_c increases by an average of 23%, indicating that combining TW and UW across multiple spans significantly enhances lighting performance. It is also worth noting that, at the 240° angle, cases with TW and UW installation show an increase in I_c—unlike the decrease observed when only UWs are used. This occurs because the TW is located close to phase A, which is the phase where the BF tends to occur.

As discussed in Section III-B, the approach combining two UWs and one TW results in a more effective reduction of overvoltages on the insulator than three UWs. Fig. 16 shows the corresponding I_c values across different power

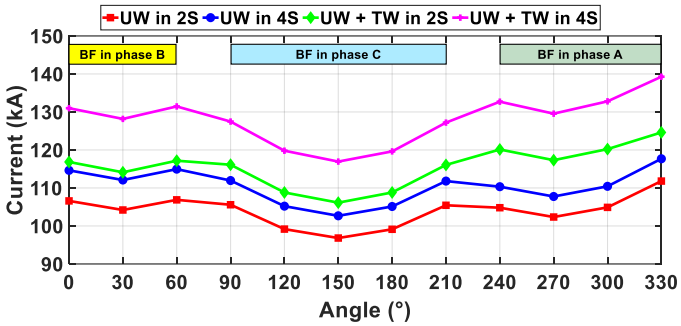

Fig. 15: I_c using TW and UW for different numbers of spans

frequency angles, with an average increase of 6.2 %. Notably, the difference between the two approaches becomes more pronounced at the 240° angle due to the presence of the TW. Furthermore, Fig. 17 illustrates the increase in I_c as the TW cross-section is enlarged, resulting in an average improvement of 5.3%.

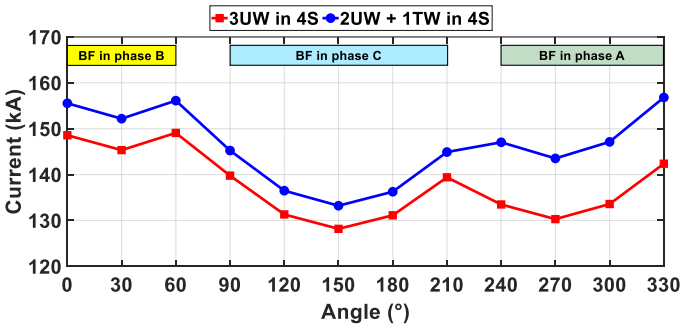

Fig. 16: I_c - Comparison between UW and TW

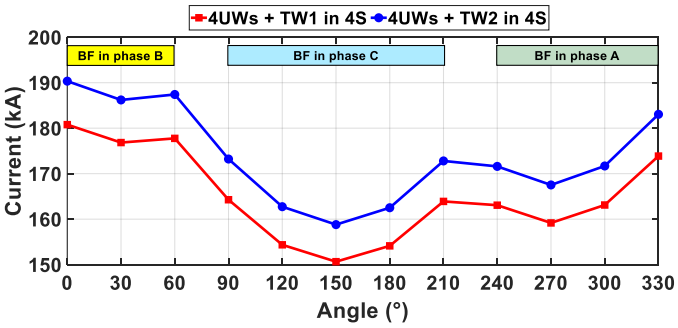

Fig. 17: I_c varying TW transversal section

Based on the critical current values (I_c), Table V summarizes the BFR and the average cumulative probability of peak lightning currents exceeding the critical current ($I_p > I_c$), following the methodology outlined in [18]. For the BFR calculation, the method recommended by CIGRÉ [1] was adopted. The parameters used include a ground flash density N_g of 1 flash/km^2/year [29], an average line attractive radius r_a of 120.8 m, and a spacing between shield wires b of 9.2 m. A simplified model for lightning stroke incidence was also employed. The implementation of UW in the OHTL reduced the BFR from 1.817 to 0.621, representing an approximate reduction of 65.8%, as it is shown in Table V. Increasing the number of spans with UW further reduced the BFR by 0.121. Moreover, combining TW and UW in two

spans decreased the BFR from 0.621 to 0.424, demonstrating improved performance. Notably, the configuration with two UWs and one TW over four spans yielded a lower BFR than three UWs across four spans. Finally, increasing the cross-sectional area of the TW resulted in a further BFR reduction of 17.8%.

TABLE V: Backflashover rate calculation for cases under analysis

Cases	$I_p > I_c$ (%)	BFR (Outages/100-km/yr)
No UW	12.08	1.817
UW in 2S	4.13	0.621
UW in 4S	3.32	0.500
UW + TW in 2S	2.82	0.424
UW + TW in 4S	1.93	0.291
3UWs in 4S	1.47	0.222
2UWs + TW in 4S	1.18	0.178
4UWs + TW1 in 4S	0.75	0.113
4UWs + TW2 in 4S	0.62	0.093

IV. Conclusions

This paper evaluated the implementation of top wire (TW) and multiple underbuilt wires (UWs) in a 220 kV single-circuit overhead transmission line (OHTL) showing the improvement in terms of reducing overvoltages and BFR. The study considered a high electrical resistivity of the ground and its frequency-dependent characteristics. The results indicate that installing UWs across several spans is ineffective. Instead, two viable options were discussed to improve BFR and overvoltages in the insulator string. The first option is to install multiple UWs, in bundle configuration, across just four spans, while the second option combines both types of wires (TW and UW). Both solutions effectively reduce the impact area and limit the number of towers affected. However, the combined option demonstrates superior performance, yielding better overall results. It was found that increasing the cross-section of the UWs is unnecessary and could have negative consequences from a civil and structural perspective. The reduction in overvoltages achieved by increasing the cross-section is negligible, while the additional mechanical load could unnecessarily stress the towers. On the other hand, better performance was observed when the cross-section of the TWs was increased.

V. References

[1] CIGRE Working Group C4.23, "Procedures for Estimating the Lightning Performance of Transmission Lines – New Aspects," p. 111, 2021.

[2] S. Visacro and F. H. Silveira, "Review of measures to improve the lightning performance of transmission lines," *Electric Power Systems Research*, vol. 213, p. 108729, 2022.

[3] M. S. Banjanin, "Application possibilities of special lightning protection systems of overhead distribution and transmission lines," *International Journal of Electrical Power & Energy Systems*, vol. 100, pp. 482–488, 2018.

[4] C. H. Moreira, F. H. Silveira, L. L. Bittencourt, and S. Visacro, "Technical-economic analysis of conventional and non-conventional techniques to improve the lightning performance of transmission lines: Extended counterpoise grounding wires and underbuilt wires," *Electric Power Systems Research*, vol. 214, p. 108805, 2023.

[5] J. E. G. Asorza, J. S. Colqui, and J. P. Filho, "Electromechanical analysis of underbuilt wire use in transmission lines," *Electric Power Systems Research*, vol. 240, p. 111282, 2025.

[6] P. Pettersson, "Propagation of waves on a wire above a lossy ground-different formulations with approximations," *IEEE Transactions on Power Delivery*, vol. 14, no. 3, pp. 1173–1180, 1999.

[7] A. C. Lima, R. A. Moura, M. A. O. Schroeder, and M. T. Correia de Barros, "Assessment of different formulations for the ground return parameters in modeling overhead lines," *Electric Power Systems Research*, vol. 164, pp. 20–30, 2018.

[8] J. S. L Colqui, R. A. R Moura, M. A. O Schroeder, J. P. Filho, and S. Kurokawa, "The impact of transmission line modeling on lightning overvoltage," *Energies*, vol. 16, no. 3, 2023.

[9] J. E. Guevara, J. S. L. Colqui, and J. P. Filho, "Analysis of overvoltage and backflashover with different transmission line models," in *SoutheastCon 2024*, 2024, pp. 498–503.

[10] CIGRE Working Group C4.33, "Impact of soil-parameter frequency dependence on the response of grounding electrodes and on the lightning performance of electrical systems," p. 67, 2019.

[11] R. Alipio and S. Visacro, "Modeling the frequency dependence of electrical parameters of soil," *IEEE Transactions on Electromagnetic Compatibility*, vol. 56, no. 5, pp. 1163–1171, 2014.

[12] A. De Conti, S. Visacro, A. Soares, and M. Schroeder, "Revision, extension, and validation of jordan's formula to calculate the surge impedance of vertical conductors," *IEEE Transactions on Electromagnetic Compatibility*, vol. 48, no. 3, pp. 530–536, 2006.

[13] F. S. Almeida, F. H. Silveira, A. De Conti, and S. Visacro, "Influence of tower modeling on the assessment of backflashover occurrence on transmission lines due to first negative lightning strokes," *Electric Power Systems Research*, vol. 197, p. 107307, 2021.

[14] S. Visacro and A. Soares, "HEM: A model for simulation of lightning-related engineering problems," *IEEE Transactions on Power Delivery*, vol. 20, no. 2 I, pp. 1206–1208, 2005.

[15] "Modeling guidelines for fast front transients," *IEEE Transactions on Power Delivery*, vol. 11, no. 1, pp. 493–506, 1996.

[16] "A simplified method for estimating lightning performance of transmission lines," *IEEE Transactions on Power Apparatus and Systems*, vol. PAS-104, no. 4, pp. 918–932, 1985.

[17] A. De Conti and S. Visacro, "Analytical representation of single- and double-peaked lightning current waveforms," *IEEE Transactions on Electromagnetic Compatibility*, vol. 49, no. 2, pp. 448–451, 2007.

[18] S. Visacro, A. Soares Jr., M. A. O. Schroeder, L. C. L. Cherchiglia, and V. J. de Sousa, "Statistical analysis of lightning current parameters: Measurements at morro do cachimbo station," *Journal of Geophysical Research: Atmospheres*, vol. 109, no. D1, 2004.

[19] Pscad simulation software. Accessed 2024-09-30.

[20] A. Morched, B. Gustavsen, and M. Tartibi, "A universal model for accurate calculation of electromagnetic transients on overhead lines and underground cables," *IEEE Transactions on Power Delivery*, vol. 14, no. 3, pp. 1032–1038, 1999.

[21] N. Zawani, Junainah, Imran, and M. Faizuhar, "Modelling of 132kv overhead transmission lines by using atp/emtp for shielding failure pattern recognition," *Procedia Engineering*, vol. 53, pp. 278–287, 2013, malaysian Technical Universities Conference on Engineering & Technology 2012, MUCET 2012.

[22] M. Qais and U. Khaled, "Evaluation of v–t characteristics caused by lightning strokes at different locations along transmission lines," *Journal of King Saud University - Engineering Sciences*, vol. 30, no. 2, pp. 150–160, 2018.

[23] Z. G. Datsios, P. N. Mikropoulos, and T. E. Tsovilis, "Evaluation of the backflashover performance of 150 kv and 400 kv double-circuit overhead transmission lines as affected by lightning attachment models and peak current distributions," *Electric Power Systems Research*, vol. 235, p. 110839, 2024.

[24] S. Company, *Southwire Overhead Conductor Manual*. Southwire, 2007.

[25] IEC 60071-1, "Insulation co-ordination – part 1: Definitions, principles and rules," Standard, 2011.

[26] IEC 60071-2, "Insulation co-ordination – part 2: Application guide," Standard, 1996.

[27] CIGRE Working Group B2.06, "Tower Top Geometry and Mid Span Clearances," p. 111, 2008.

[28] "PLS-CADD Version 16.2, Power Line Systems Inc." 2019.

[29] Z. G. Datsios, E. Stracqualursi, D. G. Patsalis, R. Araneo, P. N. Mikropoulos, and T. E. Tsovilis, "Evaluation of the backflashover performance of a 150 kv overhead transmission line considering frequency- and current-dependent effects of tower grounding systems," *IEEE Transactions on Industry Applications*, vol. 60, no. 2, pp. 2611–2620, 2024.